Research Square

Preprints are preliminary reports that have not undergone peer review.
They should not be considered conclusive, used to inform clinical practice,
or referenced by the media as validated information.

Effects of transverse-arch compression socks on ankle gear ratio and metatarsophalangeal joint energetics during running: a balanced crossover study

Honglei Liu
Liaocheng University
Chenbin Xie
Shaanxi University of Science and Technology
Wei Wang
Shanghai University of Sport
Shutao Wei
361° (China) Co., Ltd
Liwei Deng
Liaocheng University
Jiale Zhao
Universiti Malaya
Guanhong Peng
Liaocheng University
Ruixi Zheng
Xiamen University of Technology
Yong Wang
bihai_zhixin@163.com

Liaocheng University

Research Article

Keywords: compression socks, transverse arch, ankle gear ratio, metatarsophalangeal joint, running biomechanics

Posted Date: November 12th, 2026

DOI: https://doi.org/10.21203/rs.3.rs-10681246/v1

License: This work is licensed under a Creative Commons Attribution 4.0 International License. Read Full License

Additional Declarations: Competing interest reported. SW is affiliated with 361° (China) Co., Ltd. The company provided the experimental socks and access to the 361° Human Factors and Ergonomics Laboratory. Apart

from SW's contributions described in the Authors' contributions section, the company had no additional role in the study design; data collection, analysis, or interpretation; preparation of the manuscript; or the decision to submit the manuscript for publication. The other authors declare that they have no competing interests.

Abstract

Background

The transverse arch may regulate longitudinal foot stiffness through cross-axis coupling, but whether this mechanism can be translated into functional compression socks is unknown. This study examined the acute effects of transverse-arch compression socks on foot–ankle biomechanics at two running speeds.

Methods

In a balanced crossover study, 24 healthy male recreational runners completed overground running trials at 12 and 20 km/h while wearing non-compression control socks (NCS) and transverse-arch compression socks (TACS). Spatiotemporal variables and metatarsophalangeal (MTP) and ankle kinematics, kinetics, work, angular stiffness, moment arms, and gear ratio were analyzed using 2 × 2 within-subject repeated-measures analyses of variance with Bonferroni-adjusted paired comparisons for significant interactions.

Results

Significant sock × speed interactions were observed for step length ($p = 0.038$), MTP positive work ($p = 0.049$), and peak ankle plantarflexion angular velocity ($p = 0.005$). At 12 km/h, TACS increased step length (adjusted $p = 0.008$, $dz = 0.656$) and peak ankle plantarflexion angular velocity (adjusted $p = 0.024$, $dz = 0.557$); MTP positive work increased at both 12 and 20 km/h (adjusted $p = 0.007$ and 0.024; $dz = 0.662$ and 0.557, respectively). Across speeds, TACS increased stance time ($p = 0.002$) and reduced step frequency ($p = 0.016$). TACS increased MTP dorsiflexion range of motion ($p < 0.001$), peak internal plantarflexion moment ($p = 0.002$), negative work ($p = 0.002$), and net energy absorption ($p = 0.005$), without changing angular stiffness ($p = 0.241$). At the ankle, TACS increased the external moment arm ($p < 0.001$), peak gear ratio ($p = 0.001$), peak internal plantarflexion moment ($p = 0.010$), and peak power ($p = 0.025$), while the internal moment arm was unchanged ($p = 0.289$).

Conclusions

TACS acutely altered foot–ankle mechanical behavior by increasing ankle leverage and redistributing mechanical work toward greater MTP energy absorption rather than increasing MTP angular stiffness. Most effects were consistent across speeds, with no uniform evidence of speed dependence.

Trial registration:

Not applicable.

Background

During the stance phase of running, the human foot does not function as a passive rigid lever [1, 2]. Instead, it absorbs mechanical energy during early stance through arch deformation [3, 4] and metatarsophalangeal (MTP)

joint dorsiflexion [5], and then increases stiffness during propulsion to transmit forces generated by the ankle plantarflexors to the ground [6–8]. Longitudinal bending stiffness determines the extent to which the arch deforms under external loading [1, 3], and an appropriate level of stiffness helps maintain structural stability and transmit power through the distal limb [4, 6].

Previous studies have attributed longitudinal foot stiffness primarily to the bony geometry of the medial longitudinal arch, passive tension in the plantar fascia and ligaments [1, 2, 8], and active regulation by the foot muscles [3, 4, 7]. However, the transverse curvature of the forefoot is also an important structural determinant of longitudinal stiffness. Venkadesan et al. [9] demonstrated that the transverse arch contributes more than 40% of the foot's longitudinal bending stiffness through cross-axis coupling. Based on this curvature–stiffness relationship, circumferential compression around the transverse arch may help preserve transverse curvature and thereby modify longitudinal load-bearing behavior [9], with potential consequences for the lever function of the foot–ankle system [10–12].

A recent study showed that wrapping the transverse arch with an elastic band increased the ankle gear ratio and improved running economy [13], providing preliminary evidence that cross-axis coupling can be used to enhance foot–ankle lever function. However, that study used a fixed speed on a force-instrumented treadmill. It therefore remains unclear whether this mechanism produces similar biomechanical effects when translated into wearable functional socks during overground running. Moreover, increasing running speed has been shown to substantially change MTP joint angular stiffness [14], ankle moment and power demands [15–18], suggesting that the same transverse-arch compression may have different effects during moderate and fast running.

Therefore, this study compared non-compression control socks (NCS) and transverse-arch compression socks (TACS) with respect to spatiotemporal parameters and MTP and ankle joint biomechanics at two running speeds. We hypothesized that transverse-arch compression would enhance foot–ankle lever function, primarily reflected by an increase in peak ankle gear ratio. Because the effects of transverse-arch compression on MTP joint mechanics remain unclear, MTP kinematics, kinetics, and mechanical work were examined as secondary outcomes. We further examined whether these biomechanical effects differed between moderate- and fast-running speeds.

Methods

Participants

To standardize the location and tensile state of compression over the forefoot transverse arch, participants' foot size and arch morphology were restricted. Twenty-four healthy male recreational runners were enrolled. The inclusion criteria were as follows: European shoe size 42; foot length, 255–265 mm; arch height index (AHI), 0.275–0.356; body mass index, 18.5–24.9 kg/m²; weekly running distance of at least 10 km; habitual rearfoot strike pattern; and no neuromuscular, vestibular, or visual disorder that could affect running. Participant characteristics and foot morphology are summarized in Table 1. The sample size estimation was performed using G*Power 3.1 [19]. Peak ankle gear ratio was selected as the primary outcome. Based on the pilot data, the TACS–NCS difference in peak ankle gear ratio was calculated for each participant by averaging the paired differences across the two speed conditions. A priori power analysis was then conducted using a two-sided paired-samples t-test (Cohen's d_z = 0.70, α = 0.05, power = 0.80), indicating that at least 19 analyzable

participants were required. The study was conducted in accordance with the Declaration of Helsinki and approved by the Ethics Committee of Liaocheng University (HE2025101702). All participants provided written informed consent before participation.

Table 1
Participant characteristics and foot morphology.

Variable	Mean ± SD
Height (cm)	179.25 ± 4.18
Body mass (kg)	71.63 ± 4.99
Age (years)	21.29 ± 1.43
Foot length (mm)	260.83 ± 3.68
Forefoot width (mm)	97.63 ± 2.52
Forefoot girth (mm)	243.08 ± 5.92
Dorsum height (mm)	68.88 ± 2.40
AHI	0.342 ± 0.010

Note: Data are presented as mean ± standard deviation. AHI, arch height index (dorsum height at 50% of foot length/measured truncated foot length).

Sock conditions

The two socks were identical in base material, knitting process, and overall dimensions and differed only in the transverse-arch region. TACS incorporated a 50-mm-wide high-compression knitted band around the forefoot transverse arch to provide circumferential compression. NCS differed from TACS only in the absence of this band, while the yarn composition, sole length, sock height, and cuff structure were otherwise matched (Fig. 1A,B). All participants completed trials in new experimental socks and the same shoes (adidas Ultraboost 1.0, made in Vietnam).

Mechanical characterization of the experimental socks

A uniaxial tensile test was used to characterize the load-extension behavior of the transverse-arch compression band of the sock. Specimens measured 100 mm × 50 mm, with 10 mm clamped at each end and an initial gauge length of 80 mm. After applying a 0.5 N preload, displacement was zeroed and the specimens were stretched at 100 mm/min. Five specimens were tested for each sock condition (Fig. 1C). The initial circumference of the transverse-arch compression region was 160 mm. Based on the reported forefoot girth of adult men (240–270 mm) [20–22], the simulated wearing condition represented a circumferential deformation of 50.0%–68.75%, corresponding to a 40–55 mm extension of the 80-mm effective gauge length on one side. Within this range, the load was 5.05–6.34 N for NCS and 24.58–31.49 N for TACS, approximately 4.9–5.0 times that of NCS (Fig. 1D).

Experimental protocol

Experimental protocol
All trials were conducted on a 50 m indoor runway in the 361° Human Factors and Ergonomics Laboratory. Participants first underwent body and foot morphology measurements. During sock fitting, the staff ensured that the compression band was positioned around the widest part of the forefoot at the level of the metatarsal heads. Retroreflective markers were attached according to the Oxford Foot Model (OFM) [23, 24]. To avoid repositioning errors caused by reattaching markers after changing socks, all foot markers were fixed to anatomically corresponding locations on the test shoe, determined from the same underlying bony landmarks [25]. The close-fitting test shoe was also expected to minimize relative motion between the foot and shoe. Participants ran at a stable speed through a 5 m test area, with running speed monitored in real time by a photoelectric timing system. A trial was considered valid if the measured speed was within ± 5% of the target speed and the target foot made full contact with the force plate [26]. Trials were also required to exhibit a continuous and natural running gait. The order of the two target speeds was counterbalanced across participants, with 12 participants completing the 12 km/h condition first and the other 12 completing the 20 km/h condition first. The sock-condition sequence across the four experimental conditions was balanced using ABBA and BAAB sequences (A = NCS; B = TACS), with 12 participants following each sequence. Accordingly, all participants completed all four sock × speed conditions. Six valid trials were collected for each sock × speed condition and averaged for statistical analysis. At least 3 min of rest was provided between consecutive trials.

Data acquisition and processing

Kinematic data were recorded at 200 Hz using a 14-camera infrared motion capture system (T40, Vicon Motion Systems Ltd., Oxford, UK) and 14-mm retroreflective markers [25]. Ground reaction force data were collected at 2000 Hz using a Kistler force plate (9287C, Kistler Instrumente AG, Winterthur, Switzerland) [25]. The systems were synchronized using Vicon Lock Lab.

Data were processed in Visual3D (v2025.07.2, C-Motion Inc., Germantown, MD, USA). The stance phase of the right limb was the primary analysis interval, with initial contact and toe-off identified using a 20 N vertical ground reaction force threshold [27, 28]. Kinematic and kinetic data were low-pass filtered using fourth-order, zero-lag Butterworth filters with cutoff frequencies of 12 and 50 Hz, respectively [27]. Foot morphology was measured using an Anthroscan Tiger three-dimensional foot scanner (Human Solutions GmbH, Kaiserslautern, Germany; accuracy, ± 1 mm) and processed in Anthroscan v3.6.2.

Biomechanical variables

The ankle joint angle was defined as the rotation of the foot segment relative to the shank segment, and the MTP joint angle as the rotation of the toe segment relative to the metatarsal segment [23]. Ankle and MTP joint moments were calculated using Newton-Euler inverse dynamics, expressed as net internal moments, and normalized to body mass [29]. The ankle analysis interval extended from initial contact to toe-off of the right limb [29]. MTP kinematic variables were calculated over the stance phase from initial contact to toe-off. Dorsiflexion range of motion was calculated over this interval. For MTP joint kinetics and mechanical work, the analysis interval began at the first frame in which the center of pressure (COP) moved anterior to the MTP joint

center in the sagittal plane and ended at toe-off. This criterion excluded the period during which the COP was posterior to the MTP joint axis, thereby reducing attribution errors in multi-segment foot inverse dynamics [29].

Joint power was calculated as the product of the sagittal-plane net internal joint moment and joint angular velocity:

$$P\left(t\right) = M\left(t\right)\omega\ \left(t\right)$$

1

Positive and negative joint work were obtained by integrating the positive and negative portions of the power curve, respectively:

$$W_{\text{pos}} = \int_{t_0}^{t_1} \max\left[P\left(t\right), 0\right]\ dt$$

2

$$W_{\text{neg}} = \int_{t_0}^{t_1} \min\left[P\left(t\right), 0\right]\ dt$$

3

Net joint work was obtained by integrating the joint power curve over the complete analysis interval:

$$W_{\text{net}} = \int_{t_0}^{t_1} P\left(t\right)\ dt = W_{\text{pos}} + W_{\text{neg}}$$

4

where *P(t)* is joint power, *M(t)* is the sagittal-plane net internal joint moment, *ω*(t) is joint angular velocity, W_{pos} is positive joint work, W_{neg} is negative joint work, and W_{net} is net joint work. Joint angular velocity was expressed in rad/s. Negative work retained its negative sign; therefore, net work was calculated as the sum of positive and negative work.

MTP joint angular stiffness was calculated as the secant slope of the joint moment–angle relationship over a predefined loading phase:

$$K = \frac{\Delta\, M_{joint}}{\Delta\, \theta_{\ joint}}$$

5

where ΔM_{joint} and $\Delta\theta_{joint}$ represent the changes in net internal MTP plantarflexion moment and MTP joint angle, respectively, between the beginning and end of the selected phase. The analysis interval extended from the onset of the continuous increase in internal MTP plantarflexion moment to the instant of peak internal plantarflexion moment, representing the primary loading phase of the MTP joint. Angular stiffness therefore

represented the average moment–angle slope over this predefined phase rather than an instantaneous stiffness measure, and strict linearity of the entire moment–angle relationship was not assumed [14].

The ankle gear ratio was calculated as follows:

$$\mathrm{Gear\ ratio} = \frac{R}{r}$$

6

where *R* is the ankle external moment arm, defined as the two-dimensional perpendicular distance in the sagittal plane from the ankle joint center to the projected line of action of the ground reaction force. The internal moment arm, *r*, was defined as the perpendicular distance from the ankle joint center to the Achilles tendon line of action. The Achilles tendon line of action was represented by a line connecting the calcaneal marker to a virtual reference point obtained by projecting the marker along the longitudinal axis of the shank to the midpoint of shank length. This approach is consistent with previous calculations of the ankle gear ratio based on external and internal moment arms [10, 11].

Statistical analysis

Statistical analyses were performed using SPSS v27.0 (IBM Corp., Armonk, NY, USA). The normality of the residuals from each repeated-measures analysis of variance model was assessed using the Shapiro-Wilk test. For paired simple-effects comparisons following a significant interaction, normality was assessed for the corresponding within-condition difference scores [30]. Because both within-subject factors had only two levels, no sphericity test was required. Results are presented as mean ± standard deviation. Participant characteristics and foot morphology were summarized descriptively. Actual running speed, spatiotemporal parameters, MTP joint outcomes, and ankle joint outcomes were analyzed using 2 × 2 within-subject repeated-measures analyses of variance. When the sock × speed interaction was significant, Bonferroni-adjusted paired comparisons were used to test simple effects. If the interaction was not significant, the main effects of sock condition and speed were interpreted. Partial eta squared (η_p^2) was reported for analyses of variance, and Cohen's d_z was reported for simple effects [31]. All tests were two-sided, with statistical significance set at $p < 0.05$.

Results

Spatiotemporal parameters

Actual running speed showed no significant main effect of sock condition [F(1,23) = 3.289, p = 0.083, ηp² = 0.125] and no significant sock × target-speed interaction [F(1,23) < 0.001, p = 0.984, ηp² < 0.001], whereas a significant main effect of target speed was observed [F(1,23) = 44793.634, p < 0.001, ηp² = 0.999] (Table 2). These results indicated that actual running speed did not systematically differ between the NCS and TACS conditions. Step length showed a significant sock × speed interaction [F(1,23) = 4.866, p = 0.038, ηp² = 0.175]. At 12 km/h, step length was significantly greater with TACS than with NCS (1.181 ± 0.061 m vs. 1.157 ± 0.052 m; adjusted p = 0.008, dz = 0.656), whereas no difference was observed at 20 km/h (adjusted p = 1.000; Fig. 2A). Significant main effects of sock condition were observed for step frequency and stance time. TACS reduced step frequency [F(1,23) = 6.744, p = 0.016, ηp² = 0.227] and increased stance time [F(1,23) = 12.874, p = 0.002,

$\eta p^2 = 0.359$] (Fig. 2B,C). No main effect of sock condition was found for duty factor ($p = 0.161$; Fig. 2D). As speed increased, stance time and duty factor decreased significantly, whereas step frequency and step length increased significantly (all $p < 0.001$; Table 2).

Table 2
Descriptive statistics and repeated-measures ANOVA results by sock condition and running speed

Variable	12 km/h		20 km/h		Sock effect	Speed effect	Interaction
	NCS	TACS	NCS	TACS	*F* / *p* / η_p^2	*F* / *p* / η_p^2	*F* / *p* / η_p^2
Actual running speed (km/h)	11.980 ± 0.240	12.011 ± 0.253	19.940 ± 0.392	19.970 ± 0.381	3.289 / 0.083 / 0.125	44793.634 / <0.001*** / 0.999	< 0.001 / 0.984 / <0.001
Step length (m)	1.157 ± 0.052	1.181 ± 0.061	1.790 ± 0.076	1.790 ± 0.071	4.748 / 0.040* / 0.171	1192.204 / <0.001*** / 0.981	4.866 / 0.038* / 0.175
Step frequency (steps·min⁻¹)	171.488 ± 6.213	169.915 ± 5.802	182.201 ± 7.459	181.400 ± 7.832	6.744 / 0.016* / 0.227	59.790 / <0.001*** / 0.722	0.945 / 0.341 / 0.039
Stance time (s)	0.225 ± 0.017	0.228 ± 0.019	0.162 ± 0.010	0.164 ± 0.013	12.874 / 0.002** / 0.359	348.953 / <0.001*** / 0.938	0.320 / 0.577 / 0.014
Duty factor (%)	32.092 ± 2.182	32.299 ± 2.436	24.520 ± 1.296	24.801 ± 1.921	2.102 / 0.161 / 0.084	273.280 / <0.001*** / 0.922	0.057 / 0.814 / 0.002
MTP positive work (J·kg⁻¹)	0.0058 ± 0.0014	0.0065 ± 0.0017	0.0084 ± 0.0017	0.0086 ± 0.0019	14.968 / <0.001*** / 0.394	51.143 / <0.001*** / 0.690	4.308 / 0.049* / 0.158
MTP negative work (J·kg⁻¹)	-0.083 ± 0.012	-0.086 ± 0.011	-0.101 ± 0.013	-0.103 ± 0.014	12.484 / 0.002** / 0.352	19.106 / <0.001*** / 0.454	1.119 / 0.301 / 0.046
MTP net work (J·kg⁻¹)	-0.077 ± 0.011	-0.079 ± 0.010	-0.093 ± 0.012	-0.095 ± 0.014	9.505 / 0.005** / 0.292	15.467 / <0.001*** / 0.402	0.503 / 0.485 / 0.021
Peak MTP dorsiflexion angle (°)	23.785 ± 4.945	24.250 ± 4.235	24.935 ± 3.035	25.004 ± 4.205	0.353 / 0.558 / 0.015	7.080 / 0.014* / 0.235	0.265 / 0.611 / 0.011
MTP dorsiflexion ROM (°)	22.439 ± 1.883	23.376 ± 1.695	23.050 ± 2.037	23.841 ± 2.250	22.176 / <0.001*** / 0.491	1.442 / 0.242 / 0.059	0.180 / 0.675 / 0.008
Peak MTP plantarflexion moment (N·m·kg⁻¹)	-0.290 ± 0.085	-0.332 ± 0.107	-0.408 ± 0.106	-0.434 ± 0.096	11.651 / 0.002** / 0.336	54.327 / <0.001*** / 0.703	0.986 / 0.331 / 0.041
MTP angular stiffness (N·m·kg⁻¹·rad⁻¹)	1.238 ± 0.388	1.263 ± 0.376	1.600 ± 0.501	1.655 ± 0.469	1.447 / 0.241 / 0.059	28.338 / <0.001*** / 0.552	0.339 / 0.566 / 0.015

Variable	12 km/h		20 km/h		Sock effect	Speed effect	Interaction
	NCS	TACS	NCS	TACS	*F* / *p* / η_p^2	*F* / *p* / η_p^2	*F* / *p* / η_p^2
Peak ankle plantarflexion angular velocity (°·s⁻¹)	-521.613 ± 57.324	-558.360 ± 59.911	-742.812 ± 47.537	-732.649 ± 50.761	2.308 / 0.142 / 0.091	258.604 / <0.001*** / 0.918	9.758 / 0.005** / 0.298
Peak ankle plantarflexion moment (N·m·kg⁻¹)	-2.669 ± 0.362	-2.835 ± 0.439	-3.371 ± 0.276	-3.420 ± 0.257	7.942 / 0.010** / 0.257	199.761 / <0.001*** / 0.897	2.311 / 0.142 / 0.091
Peak ankle power (W·kg⁻¹)	13.470 ± 2.446	14.657 ± 3.055	24.216 ± 2.740	24.591 ± 2.653	5.760 / 0.025* / 0.200	393.154 / <0.001*** / 0.945	2.001 / 0.171 / 0.080
External moment arm at peak gear ratio (cm)	16.787 ± 0.449	16.966 ± 0.558	16.747 ± 0.385	16.865 ± 0.464	18.528 / <0.001*** / 0.446	0.894 / 0.354 / 0.037	0.757 / 0.393 / 0.032
Internal moment arm at peak gear ratio (cm)	4.889 ± 0.071	4.898 ± 0.085	4.887 ± 0.081	4.887 ± 0.083	1.176 / 0.289 / 0.049	0.680 / 0.418 / 0.029	2.869 / 0.104 / 0.111
Peak ankle gear ratio	3.434 ± 0.098	3.465 ± 0.127	3.428 ± 0.112	3.453 ± 0.126	14.044 / 0.001** / 0.379	0.403 / 0.532 / 0.017	0.201 / 0.658 / 0.009

Metatarsophalangeal joint biomechanics

MTP joint positive work demonstrated a significant sock × speed interaction [$F(1,23) = 4.308$, $p = 0.049$, $\eta p^2 = 0.158$]. TACS significantly increased positive work at both 12 and 20 km/h (adjusted $p = 0.007$ and 0.024; $dz = 0.662$ and 0.557, respectively; Fig. 3A). No significant interactions were observed for the other MTP outcomes (all $p > 0.05$). Therefore, the main effects of sock condition and speed were interpreted. For the main effect of sock condition, TACS did not change peak dorsiflexion angle ($p = 0.558$; Table 2), but increased dorsiflexion range of motion [$F(1,23) = 22.176$, $p < 0.001$, $\eta p^2 = 0.491$]. TACS also resulted in a higher peak internal plantarflexion moment [$F(1,23) = 11.651$, $p = 0.002$, $\eta p^2 = 0.336$], greater negative work [$F(1,23) = 12.484$, $p = 0.002$, $\eta p^2 = 0.352$], and more negative net work [$F(1,23) = 9.505$, $p = 0.005$, $\eta p^2 = 0.292$], without affecting angular stiffness ($p = 0.241$; Fig. 3B–F). For the main effect of speed, as speed increased, peak dorsiflexion angle ($p = 0.014$), peak plantarflexion moment, angular stiffness, positive work, and negative work increased, whereas net work became more negative (all remaining $p < 0.001$). Dorsiflexion range of motion did not change significantly (Table 2).

Ankle joint biomechanics

Peak ankle plantarflexion angular velocity exhibited a significant sock × speed interaction [$F(1,23) = 9.758$, $p = 0.005$, $\eta p^2 = 0.298$]. At 12 km/h, TACS significantly increased peak ankle plantarflexion angular velocity (adjusted $p = 0.024$, $dz = 0.557$), whereas no significant difference was observed at 20 km/h (adjusted $p = 0.560$;

Fig. 4A). No significant interactions were observed for the remaining ankle outcomes (all $p > 0.05$). For the main effect of sock condition, TACS increased peak internal ankle plantarflexion moment [$F(1,23) = 7.942$, $p = 0.010$, $\eta p^2 = 0.257$] and peak ankle power [$F(1,23) = 5.760$, $p = 0.025$, $\eta p^2 = 0.200$]. TACS exhibited a larger external moment arm at the instant of peak gear ratio [$F(1,23) = 18.528$, $p < 0.001$, $\eta p^2 = 0.446$], whereas the internal moment arm remained unchanged ($p = 0.289$), accompanied by a higher peak ankle gear ratio [$F(1,23) = 14.044$, $p = 0.001$, $\eta p^2 = 0.379$] (Fig. 4B–F). The main effect of speed showed that faster speeds were associated with greater peak ankle plantarflexion moment magnitude, angular velocity, and power (all $p < 0.001$), while peak gear ratio and its internal and external moment arms were unaffected (Table 2).

Discussion

This study investigated the effects of TACS versus NCS on spatiotemporal, MTP, and ankle joint biomechanics during running at 12 and 20 km/h. TACS increased ankle gear ratio as hypothesized and was also associated with greater MTP joint mechanical energy absorption. In addition, TACS was associated with longer stance time, lower step frequency, greater peak ankle plantarflexion moment and power, and greater MTP dorsiflexion range of motion and plantarflexion moment, without a significant change in MTP angular stiffness. These effects were largely consistent across speeds, except for step length, MTP positive work, and peak ankle plantarflexion angular velocity.

Effects of TACS on spatiotemporal coordination and speed dependence

Across speeds, TACS reduced step frequency and increased stance time, while step length increased only at 12 km/h. This indicates that participants did not merely modify local joint mechanics but reorganized the overall coordination of step length, step frequency, and ground-contact time. A longer stance time may provide the ankle plantarflexors with a longer interval for force application [15]. Accordingly, the concurrent changes in spatiotemporal parameters and ankle kinetics suggest that the increases in peak ankle plantarflexion moment and power associated with TACS were part of a broader adjustment in running coordination. As speed increased from 12 to 20 km/h, stance time and duty factor decreased, whereas step frequency, step length, and most foot–ankle kinetic outcomes increased [15, 16], consistent with the higher joint loading and power demands of faster running [16–18].

Sock × speed interactions occurred for three outcomes, but their directions were not uniform. MTP positive work increased at both speeds, and the interaction primarily reflected a difference in the magnitude of increase. In contrast, significant simple effects for step length and peak ankle plantarflexion angular velocity were observed only at 12 km/h. Thus, the biomechanical effects of TACS did not show a clear overall speed specificity. Previous studies have shown that the effects of footwear longitudinal bending stiffness on joint mechanics may vary with running speed [32], although such interactions are not present for all outcomes [32, 33]. At 20 km/h, the mechanical demands on the foot–ankle system were greater, while the TACS design maintained a fixed circumferential compression level. Therefore, the relative effectiveness of transverse arch constraint may have diminished at the higher speed. This explanation remains speculative and should be verified by directly measuring transverse-arch deformation at different running speeds.

Effects of TACS on the metatarsophalangeal joint

During late stance in running, the MTP joint typically absorbs mechanical energy during dorsiflexion [5, 34], and this energy exchange is influenced by joint range of motion, moment, and stiffness [14, 34, 35]. The MTP results showed that TACS was associated with greater mechanical energy absorption. Footwear with increased longitudinal bending stiffness, including plate-based designs, can restrict MTP dorsiflexion and alter MTP joint energetics [34, 36, 37]. In contrast, TACS applied circumferential pressure around the forefoot transverse arch and did not provide longitudinal rigid support across the MTP joint axis. Consistent with this structural difference, no significant increase in MTP angular stiffness was observed with TACS. TACS also did not significantly alter peak MTP dorsiflexion angle. The circumferential compression provided by TACS may have altered forefoot posture at initial contact and thereby increased the excursion available for MTP dorsiflexion. This proposed mechanism remains speculative and should be tested by directly quantifying MTP posture at stance onset.

TACS was associated with greater MTP dorsiflexion range of motion and peak internal plantarflexion moment, which may have contributed to greater negative work and a more negative net work. Although positive work increased at both speeds, this increase was insufficient to offset the greater negative work. These findings indicate that TACS was associated with greater mechanical energy exchange at the MTP joint during late stance. Because net joint work cannot distinguish elastic energy storage and return in passive tissues, active muscular work, and energy transfer among foot segments, the present study cannot determine whether the additional negative work represented recoverable elastic energy storage or dissipative energy loss.

Effects of TACS on the ankle joint

The higher peak ankle gear ratio with TACS was primarily attributable to an increased external moment arm, whereas the internal moment arm did not change significantly. Because the external moment arm depends on the relative geometry between the ground reaction force line of action and the ankle joint center, the present findings indicate an altered external lever arm but do not by themselves demonstrate an anterior shift of the center of pressure. Previous experiments reported that transverse-arch wrapping shifted the center of pressure anteriorly and increased the ankle gear ratio during running [13], providing a plausible mechanism for the present findings.

Importantly, a higher ankle gear ratio does not imply a lower mechanical demand on the ankle plantarflexors. Across speeds, TACS was associated with greater peak ankle plantarflexion moment and peak ankle power; at 12 km/h, it was also associated with a greater magnitude of peak plantarflexion angular velocity. Together, these findings indicate greater peak joint-level mechanical demands at the ankle; however, plantarflexor muscle force was not directly measured.

Potential mechanism and functional role of TACS

Wrapping the transverse arch has been shown to influence longitudinal foot stiffness through cross-axis coupling [9, 13]. However, the present study did not directly measure transverse-arch deformation or longitudinal foot stiffness; therefore, the mechanisms underlying the observed biomechanical changes cannot be determined from the current data. The circumferential compression provided by TACS may have altered forefoot geometry, plantar load distribution, foot–shoe coupling, or sensory input, any of which could have contributed to the observed changes in ankle external moment arm and MTP joint mechanics. Accordingly, the combination of a greater ankle external moment arm and unchanged MTP angular stiffness should be

interpreted as a biomechanical response that is compatible with, but does not confirm, a stiffness-related mechanism.

Tang and Beck reported improved running economy with experimental transverse-arch wrapping [13], but their wrapping method, test speed, and treadmill condition differed from those used here. Other studies have shown that restricting longitudinal arch compression may increase metabolic cost [6], increasing footwear longitudinal bending stiffness may produce no significant improvement in running economy [38], and the effects of footwear longitudinal bending stiffness on running economy may be speed dependent [39]. Because transverse-arch deformation, plantar pressure, muscle activity, and metabolic cost were not directly measured in the present study, the mechanisms underlying the observed biomechanical changes remain to be established. The present findings therefore support acute changes in foot–ankle mechanical behavior with TACS, but do not demonstrate a specific underlying mechanism or an improvement in running economy or performance.

Limitations

This study has several limitations. First, the participants were young, healthy male rearfoot-strike runners with a narrow range of shoe sizes and arch morphology. This homogeneous sample limits generalizability to women, other foot types, other strike patterns, and clinical populations. Future studies should recruit more diverse samples to examine individual differences in the response to TACS. Second, only one compression-band configuration and band width were tested, precluding identification of a dose-response relationship. Further investigation is warranted to examine the effects of varying circumferential pressures and band widths, while controlling for material properties and overall sock construction. Third, electromyography and metabolic data were not collected, limiting interpretation of the effects on neuromuscular response and running economy. Further investigation is warranted to incorporate electromyographic and metabolic measurements to clarify the mechanisms underlying TACS-induced adaptations. Fourth, because the foot markers were attached to the shoe upper, deformation of the upper and relative foot-shoe motion may have affected the foot kinematics [25]. The reported foot kinematics should therefore be interpreted as an approximation of in-shoe foot motion. Future work could validate these measurements using shoe-window protocols or biplanar fluoroscopy.

Conclusions

TACS increased ankle gear ratio and was associated with greater peak ankle plantarflexion moment and power, but did not enhance MTP angular stiffness, instead increasing MTP mechanical energy absorption. These findings indicate that the acute effects of TACS primarily involve altered foot–ankle leverage and redistribution of mechanical work rather than a simple increase in MTP joint stiffness. Further investigation incorporating different compression configurations, neuromuscular and metabolic measurements, and diverse populations is needed to establish individualized TACS designs and their implications for running performance.

Abbreviations

TACS
Transverse-arch compression socks
NCS
Non-compression control socks
MTP

Metatarsophalangeal
AHI
Arch height index
COP
Center of pressure

Declarations

Ethics approval and consent to participate

The study was conducted in accordance with the Declaration of Helsinki and was approved by the Ethics Committee of Liaocheng University (HE2025101702; 17 October 2025). All participants provided written informed consent before participation.

Consent for publication

Not applicable.

Competing Interests

SW is affiliated with 361° (China) Co., Ltd. The company provided the experimental socks and access to the 361° Human Factors and Ergonomics Laboratory. Apart from SW's contributions described in the Authors' contributions section, the company had no additional role in the study design; data collection, analysis, or interpretation; preparation of the manuscript; or the decision to submit the manuscript for publication. The other authors declare that they have no competing interests.

Authors' information

Not applicable.

Note

Cells for sock effect, speed effect, and interaction report F(1,23), p, and ηp^2, respectively. Negative and net MTP joint work retain their algebraic signs; more negative values indicate greater mechanical energy absorption. Ankle plantarflexion moment and angular velocity are defined as negative in the study coordinate system. *p < 0.05, **p < 0.01, ***p < 0.001.

Funding

This research was funded by the Science and Technology Innovation Project of the General Administration of Sport of China (grant numbers 25KJCX106 and 24KJCX089), the Collaborative Innovation Platform Project of the Fuzhou–Xiamen–Quanzhou National Independent Innovation Demonstration Zone (grant number 2024-P-003), and the Fujian Provincial Social Science Foundation (grant number FJ2025BF039).

Author Contribution

HL and CX conceptualized the study and developed the methodology. HL, WW, and JZ conducted the formal analysis. HL, CX, WW, LD, GP, and RZ performed the investigation. SW provided resources. HL and JZ curated the data. HL and WW drafted the manuscript. YW and CX reviewed and edited the manuscript. HL prepared the visualizations. YW and SW supervised the study. All authors read and approved the final manuscript.

Acknowledgement

The authors thank all participants and the 361° Human Factors and Ergonomics Laboratory for their assistance with this study.

Data Availability

The datasets generated and/or analysed during the current study are available from the corresponding author on reasonable request.

References

1. Welte L, Kelly LA, Lichtwark GA, Rainbow MJ. Influence of the windlass mechanism on arch-spring mechanics during dynamic foot arch deformation. J R Soc Interface. 2018;15:20180270.
2. Ker RF, Bennett MB, Bibby SR, Kester RC, Alexander RM. The spring in the arch of the human foot. Nature. 1987;325:147–9.
3. Kelly LA, Cresswell AG, Racinais S, Whiteley R, Lichtwark GA. Intrinsic foot muscles have the capacity to control deformation of the longitudinal arch. J R Soc Interface. 2014;11:20131188.
4. Farris DJ, Kelly LA, Cresswell AG, Lichtwark GA. The functional importance of human foot muscles for bipedal locomotion. Proc Natl Acad Sci U S A. 2019;116:1645–50.
5. Stefanyshyn DJ, Nigg BM. Mechanical energy contribution of the metatarsophalangeal joint to running and sprinting. J Biomech. 1997;30:1081–5.
6. Stearne SM, McDonald KA, Alderson JA, North I, Oxnard CE, Rubenson J. The foot's arch and the energetics of human locomotion. Sci Rep. 2016;6:19403.
7. Kelly LA, Farris DJ, Cresswell AG, Lichtwark GA. Intrinsic foot muscles contribute to elastic energy storage and return in the human foot. J Appl Physiol (1985). 2019;126:231–238.
8. Welte L, Kelly LA, Kessler SE, Lieberman DE, D'Andrea SE, Lichtwark GA, et al. The extensibility of the plantar fascia influences the windlass mechanism during human running. Proc Biol Sci. 2021;288:20202095.
9. Venkadesan M, Yawar A, Eng CM, Dias MA, Singh DK, Tommasini SM, et al. Stiffness of the human foot and evolution of the transverse arch. Nature. 2020;579:97–100.
10. Ray SF, Takahashi KZ. Gearing up the human ankle-foot system to reduce energy cost of fast walking. Sci Rep. 2020;10:8793.
11. Takahashi KZ, Gross MT, van Werkhoven H, Piazza SJ, Sawicki GS. Adding stiffness to the foot modulates soleus force-velocity behaviour during human walking. Sci Rep. 2016;6:29870.

12. Smith R, Lichtwark G, Farris D, Kelly L. Examining the intrinsic foot muscles' capacity to modulate plantar flexor gearing and ankle joint contributions to propulsion in vertical jumping. J Sport Health Sci. 2023;12:639–47.
13. Tang H, Beck ON. Wrapping the transverse foot arch improves running economy. J Exp Biol. 2025;228:jeb250566.
14. Day EM, Hahn ME. Dynamic angular stiffness about the metatarsophalangeal joint increases with running speed. Hum Mov Sci. 2019;67:102501.
15. Orendurff MS, Kobayashi T, Tulchin-Francis K, Tullock AMH, Villarosa C, Chan C, et al. A little bit faster: lower extremity joint kinematics and kinetics as recreational runners achieve faster speeds. J Biomech. 2018;71:167–75.
16. Schache AG, Blanch PD, Dorn TW, Brown NAT, Rosemond D, Pandy MG. Effect of running speed on lower limb joint kinetics. Med Sci Sports Exerc. 2011;43:1260–71.
17. Lai A, Schache AG, Brown NAT, Pandy MG. Human ankle plantar flexor muscle-tendon mechanics and energetics during maximum acceleration sprinting. J R Soc Interface. 2016;13:20160391.
18. Werkhausen A, Cronin NJ, Albracht K, Bojsen-Møller J, Seynnes OR. Distinct muscle-tendon interaction during running at different speeds and in different loading conditions. J Appl Physiol (1985). 2019;127:246–253.
19. Faul F, Erdfelder E, Lang AG, Buchner A. G*Power 3: a flexible statistical power analysis program for the social, behavioral, and biomedical sciences. Behav Res Methods. 2007;39:175–91.
20. Cao B, Wang J, Shi W, Lu X, Zhou K. 3D foot anthropometric measurements under two weight-bearing conditions for ergonomic design of foot-related products. Int J Morphol. 2023;41:1209–18.
21. Mo S, Lu F, Li C, Zhao H. Effects of 10 KM run on foot morphology and bilateral symmetry in male recreational runners. Front Bioeng Biotechnol. 2024;12:1427418.
22. Hajaghazadeh M, Emamgholizadeh Minaei R, Allahyari T, Khalkhali H. Anthropometric dimensions of the foot in northwestern Iran and comparison with other populations. Health Scope. 2018;7:e14063.
23. Carson MC, Harrington ME, Thompson N, O'Connor JJ, Theologis TN. Kinematic analysis of a multi-segment foot model for research and clinical applications: a repeatability analysis. J Biomech. 2001;34:1299–307.
24. Wright CJ, Arnold BL, Coffey TG, Pidcoe PE. Repeatability of the modified Oxford Foot Model during gait in healthy adults. Gait Posture. 2011;33:108–12.
25. Perrin TP, Morio CYM, Besson T, Kerhervé HA, Millet GY, Rossi J. Comparison of skin and shoe marker placement on metatarsophalangeal joint kinematics and kinetics during running. J Biomech. 2023;146:111410.
26. Fu F, Guo L, Tang X, Wang J, Xie Z, Fekete G, et al. Effect of the innovative running shoes with the special midsole structure on the female runners' lower limb biomechanics. Front Bioeng Biotechnol. 2022;10:866321.
27. Wang IL, Graham RB, Bourdon EJP, Chen YM, Gu CY, Wang LI. Biomechanical analysis of running foot strike in shoes of different mass. J Sports Sci Med. 2020;19:130–7.
28. Fellin RE, Rose WC, Royer TD, Davis IS. Comparison of methods for kinematic identification of footstrike and toe-off during overground and treadmill running. J Sci Med Sport. 2010;13:646–50.

29. Bruening DA, Takahashi KZ. Partitioning ground reaction forces for multi-segment foot joint kinetics. Gait Posture. 2018;62:111–6.
30. Shapiro SS, Wilk MB. An analysis of variance test for normality (complete samples). Biometrika. 1965;52:591–611.
31. Lakens D. Calculating and reporting effect sizes to facilitate cumulative science: a practical primer for t-tests and ANOVAs. Front Psychol. 2013;4:863.
32. Day EM, Hahn ME. Does running speed affect the response of joint level mechanics in non-rearfoot strike runners to footwear of varying longitudinal bending stiffness? Gait Posture. 2021;84:187–91.
33. Kiesewetter P, Milani TL, Mitschke C. Running velocity as a methodological factor in footwear testing: fixed versus self-selected conditions. Bioeng (Basel). 2026;13:751.
34. Willwacher S, König M, Potthast W, Brüggemann GP. Does specific footwear facilitate energy storage and return at the metatarsophalangeal joint in running? J Appl Biomech. 2013;29:583–92.
35. Cigoja S, Firminger CR, Asmussen MJ, Fletcher JR, Edwards WB, Nigg BM. Does increased midsole bending stiffness of sport shoes redistribute lower limb joint work during running? J Sci Med Sport. 2019;22:1272–7.
36. Oh K, Park S. The bending stiffness of shoes is beneficial to running energetics if it does not disturb natural MTP joint flexion. J Biomech. 2017;53:127–35.
37. Stefanyshyn DJ, Nigg BM. Influence of midsole bending stiffness on joint energy and jump height performance. Med Sci Sports Exerc. 2000;32:471–6.
38. Healey LA, Hoogkamer W. Longitudinal bending stiffness does not affect running economy in Nike Vaporfly shoes. J Sport Health Sci. 2022;11:285–92.
39. Day EM, Hahn ME. Optimal footwear longitudinal bending stiffness to improve running economy is speed dependent. Footwear Sci. 2020;12:3–13.

Figures

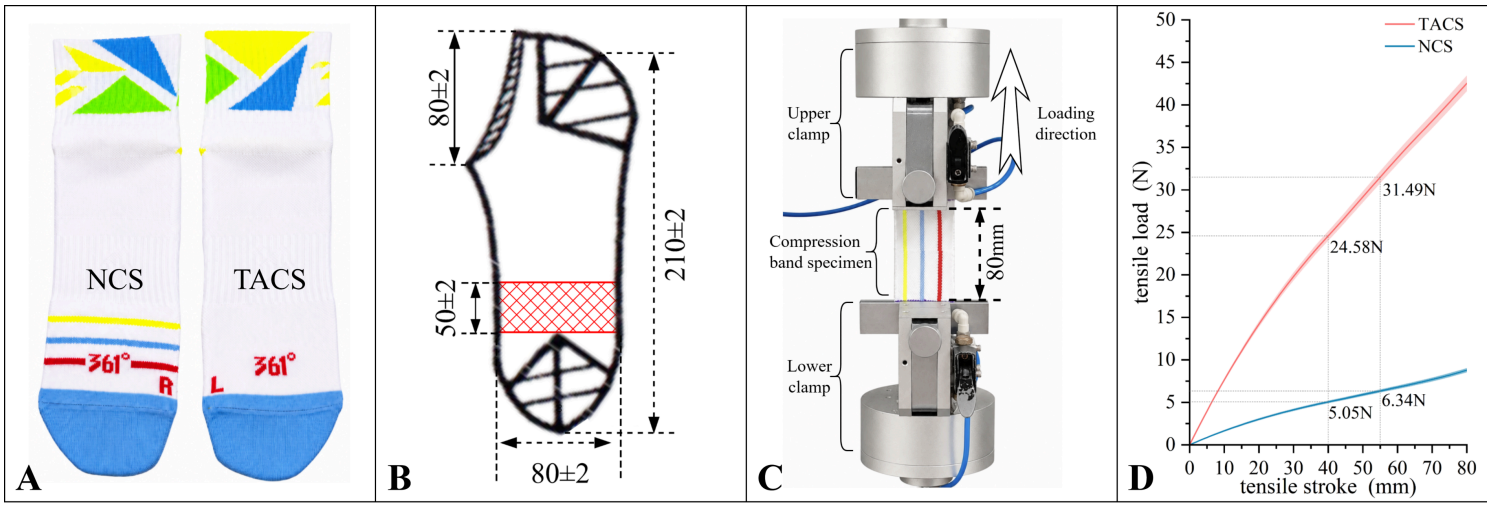


Figure 1

Experimental sock design and mechanical characterization. (A) Appearance of the experimental and control socks; (B) compression sock construction and dimensions (mm; manufacturing tolerance, ±2 mm); (C) uniaxial tensile test of the specimen in the transverse-arch region; (D) load-extension curves of the experimental socks from 0 to 80 mm.

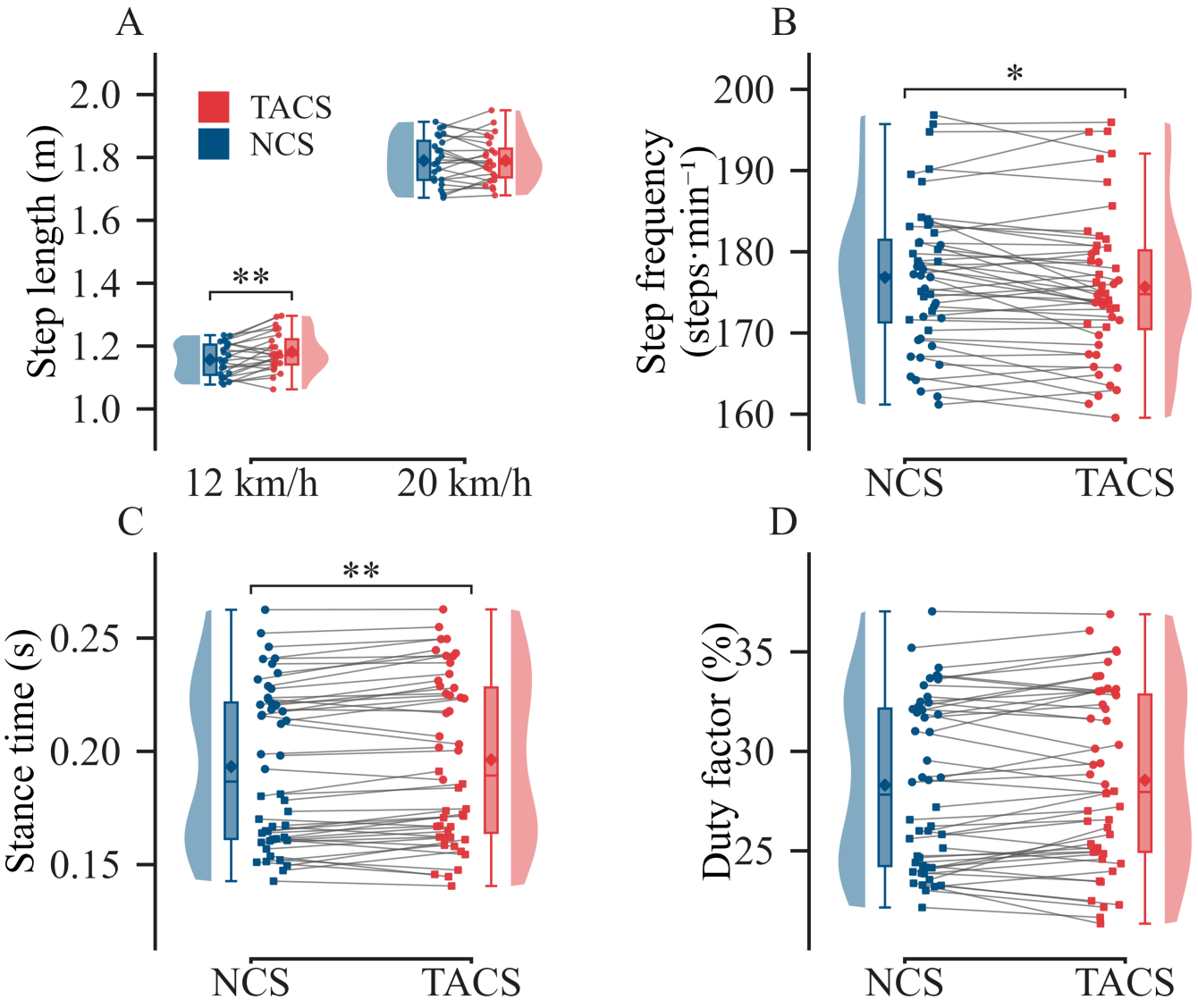


Figure 2

Effects of transverse-arch compression socks on spatiotemporal parameters. (A) Step length; (B) step frequency (120/gait-cycle duration); (C) stance time; (D) duty factor (stance time/gait-cycle duration × 100%). Data are displayed as raincloud plots. The half-violin plots show the kernel density distributions, individual observations, the 25th–75th percentiles (boxes), medians (horizontal lines within the boxes), means (diamonds), and whiskers extending to the most extreme observations within 1.5 × the interquartile range (IQR). Gray lines connect data from the same participant under NCS and TACS conditions. Circles indicate 12 km/h and squares denote 20 km/h. *p < 0.05, **p < 0.01, ***p < 0.001.

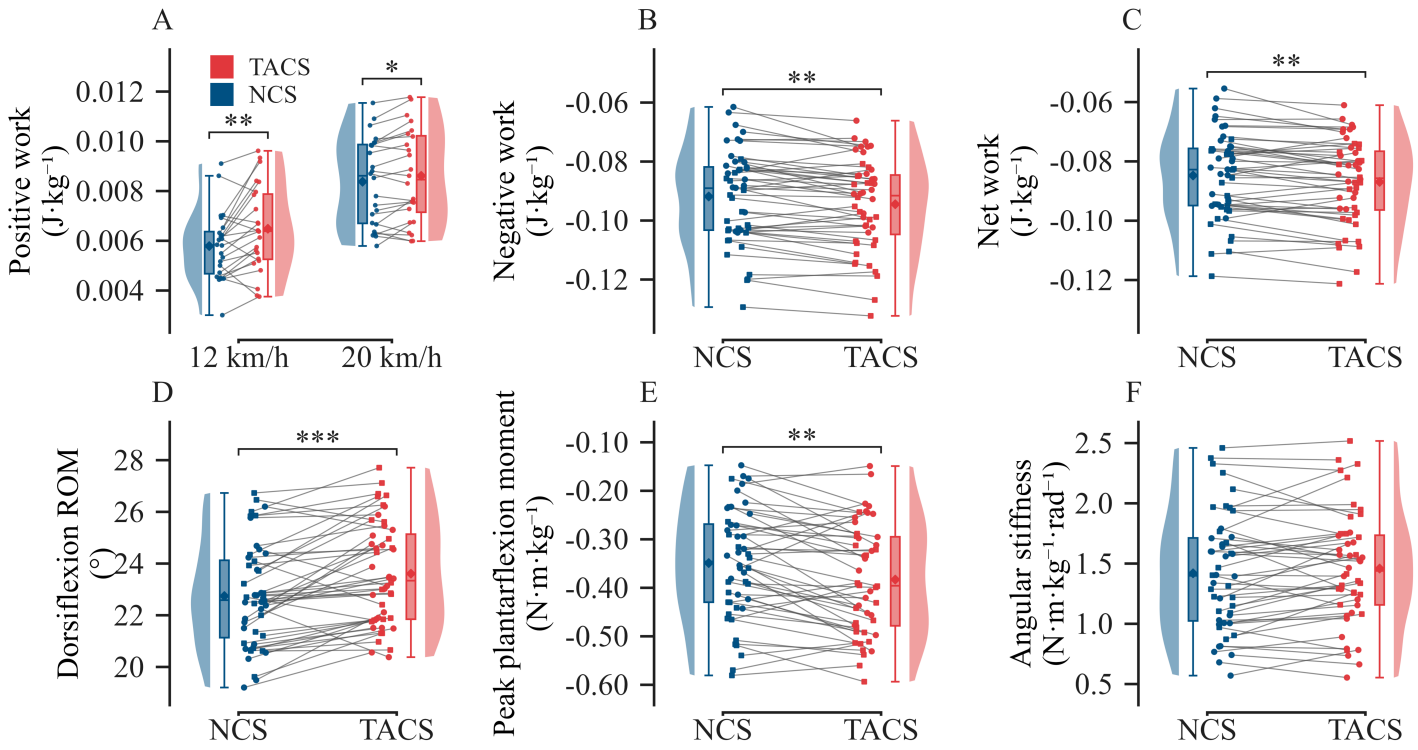


Figure 3

Effects of transverse-arch compression socks on MTP joint biomechanics. (A) Positive work; (B) negative work; (C) net work; (D) dorsiflexion range of motion; (E) peak plantarflexion moment; (F) angular stiffness. Data are displayed as raincloud plots. Half-violin plots show the kernel density distributions (violins), individual observations (points), the 25th–75th percentiles (boxes), medians (horizontal lines within the boxes), means (diamonds), and whiskers extending to the most extreme observations within 1.5 × the interquartile range (IQR) below the first quartile and above the third quartile. Gray lines connect data from the same participant under NCS and TACS conditions. Circles indicate 12 km/h and squares indicate 20 km/h. *p < 0.05, **p < 0.01, ***p < 0.001.

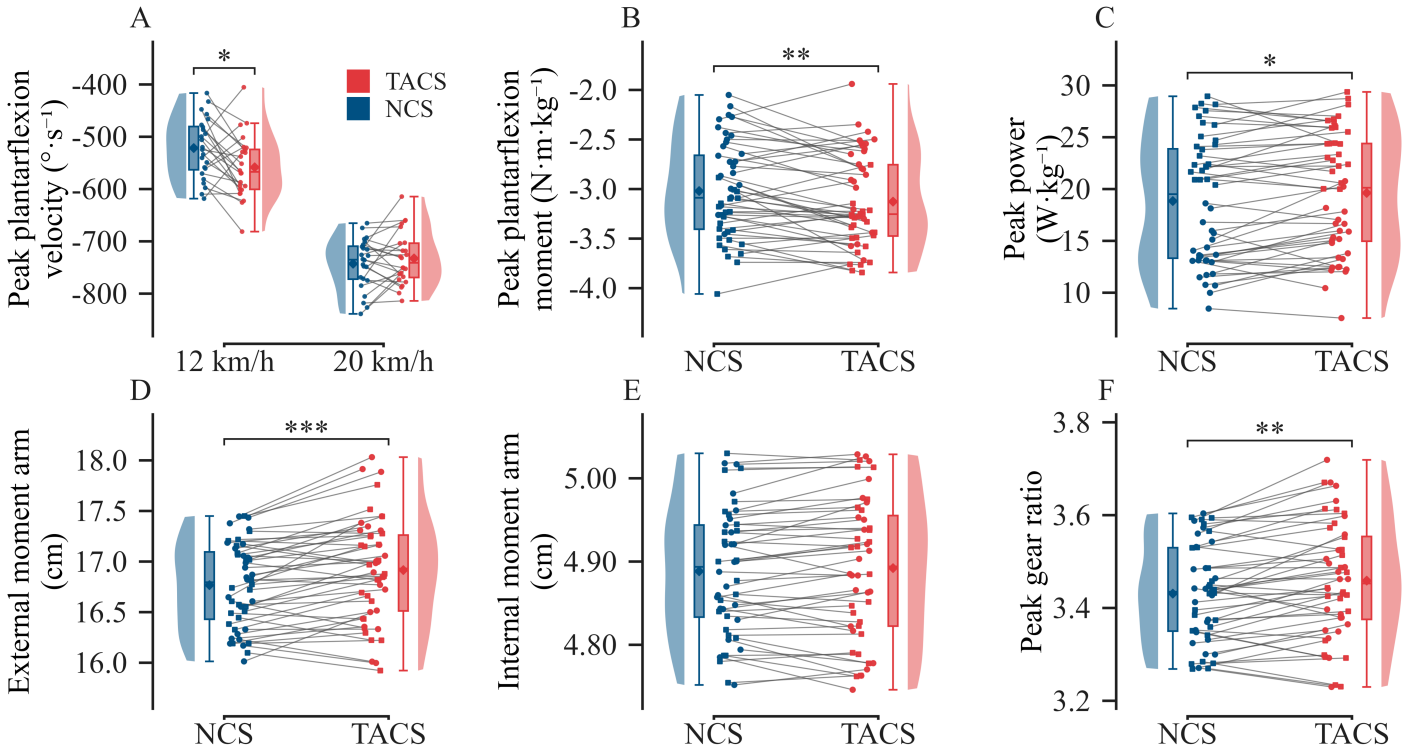


Figure 4

Effects of transverse-arch compression socks on ankle joint kinetics and gear-ratio variables at different running speeds. (A) Peak ankle plantarflexion angular velocity; (B) peak ankle plantarflexion moment; (C) peak ankle power; (D) external moment arm at peak gear ratio; (E) internal moment arm at peak gear ratio; (F) peak ankle gear ratio. Data are displayed as raincloud plots. Half-violin plots show kernel density distributions, points show individual observations, boxes indicate the 25th–75th percentiles, horizontal lines within boxes indicate medians, diamonds indicate means, and whiskers extend to the minimum and maximum values within 1.5 times the interquartile range below the first quartile and above the third quartile. Gray lines connect data from the same participant under NCS and TACS conditions. Circles indicate 12 km/h and squares indicate 20 km/h. *p < 0.05, **p < 0.01, ***p < 0.001.